Available online at www.sciencedirect.com
ScienceDirect
Catalysis Today 129 (2007) 346–354
CATALYSIS TODAY
www.elsevier.com/locate/cattod

Investigation of bio-ethanol steam reforming over cobalt-based catalysts

Hua Song, Lingzhi Zhang, Rick B. Watson, Drew Braden, Umit S. Ozkan *

Heterogeneous Catalysis Research Group, Department of Chemical & Biomolecular Engineering, The Ohio State University, Columbus, OH 43210, USA

Available online 20 September 2007

Abstract

The catalytic performance of cobalt catalysts supported on γ-Al_2O_3, TiO_2, ZrO_2 were studied for bio-ethanol steam reforming (BESR) reaction. The supported catalysts (10 wt%Co) were prepared by impregnation and characterized through Thermogravimetric analysis (TGA), H_2 chemisorption, laser Raman Spectroscopy, Diffuse Reflectance Infrared Fourier Transform Spectroscopy (DRIFTS), and temperature-programmed reaction (TPRxn). The metallic cobalt sites were found to correlate with the BESR reaction activity. The reaction and H_2 chemisorption showed that ZrO_2 supported catalyst showed the best dispersion and best catalytic activity. Over the 10% Co/ZrO_2 catalyst, using a H_2O:EtOH:inert molar ratio of 10:1:75 and a GHSV = 5000 h^{-1}, 100% ethanol conversion and a yield of 5.5 mol H_2/mol EtOH were obtained at 550 °C and atmospheric pressure.

Keywords: Cobalt catalyst; Zirconia; Alumina; Titania; Bio-ethanol steam reforming; TGA; H_2 chemisorption; Raman; DRIFTS; Temperature-programmed reaction

1. Introduction

Hydrogen energy is likely to play a major role as a primary energy carrier for the future. It provides a clean energy source since it burns without emitting any environmental pollutants. With increased interest and rapid developments in fuel cell technology, hydrogen has attracted further attention as a fuel for fuel cells. Hydrogen production from fossil fuels has been investigated for many years. However, fossil fuel is not a sustainable energy source. For hydrogen to fulfill its potential as a primary energy carrier of the future, new technologies that can produce hydrogen from renewable sources are needed. One highly attractive route for hydrogen production is steam reforming of bio-ethanol. Bio-ethanol can be obtained from biomass fermentation. In theory, hydrogen production from biomass or biomass-derived liquids can be a carbon-emission free process since all carbon dioxide produced can be recycled back to the plants using solar energy. Hydrogen production from bio-ethanol through steam reforming also has the potential to resolve many of the issues involved in hydrogen storage and hydrogen delivery infrastructure and lends itself very well to a distributed hydrogen production strategy. Currently there is no commercial catalyst for bio-ethanol reforming. In addition, many fundamental questions in catalytic reforming of ethanol still remain, such as the nature of active sites, the network of competing reactions, and catalyst deactivation.

Hydrogen can be produced from ethanol through a seemingly straightforward steam reforming reaction

$$C_2H_5OH_{(l)} + 3H_2O_{(l)} \rightarrow 2CO_2 + 6H_2 \qquad (\Delta H_r = 348\ \text{kJ/mol at } 25\,^\circ\text{C})$$

This reaction is endothermic and would require energy input. Although the products from the desired reactions are only CO_2 and H_2, in reality, depending on the reaction conditions and catalysts used, the product distribution can be governed by a very complex reaction network. Possible reactions involved can be as follows.

$$CH_3CH_2OH \rightarrow CH_4 + CO + H_2 \qquad \text{(ethanol decomposition)}$$

$$CH_3CH_2OH \rightarrow CH_3CHO + H_2 \qquad \text{(dehydrogenation)}$$

$$CH_3CH_2OH \rightarrow C_2H_4 + H_2O \qquad \text{(dehydration)}$$

$$CH_3CH_2OH + H_2O \rightarrow 2CO + 4H_2 \qquad \text{(incomplete reforming)}$$

$$2CH_3CH_2OH \rightarrow (C_2H_5)_2O + H_2O \qquad \text{(dehydrative coupling)}$$

$$CO + 3H_2 \rightarrow CH_4 + H_2O \qquad \text{(methanation)}$$

* Corresponding author. Tel.: +1 614 292 6623.
E-mail address: Ozkan.1@osu.edu (U.S. Ozkan).

0920-5861/$ – see front matter
doi:10.1016/j.cattod.2006.11.028

$$CH_4 + 2H_2O \rightarrow CO_2 + 4H_2 \quad \text{(steam reforming)}$$

$$CO + H_2O \leftrightarrows CO_2 + H_2 \quad \text{(water-gas shift)}$$

$$2CO \rightarrow CO_2 + C \quad \text{(Boudouard reaction)}$$

There are many side reactions that might take place during ethanol steam reforming, complicating the product distribution. To get the highest possible H_2 yield for industrial applications, it is essential to investigate the effects of temperature, reactants ratio, pressure, space velocity as well as the catalytic parameters. A thermodynamic analysis was performed using the software HSC®5.1. All possible products, including solid carbon were included among the possible species that could exist in the equilibrium state.

In the thermodynamic analysis, the following definitions are used.

$$H_2\text{Yield}\% = \frac{\text{moles of } H_2 \text{ produced}}{6 \times (\text{moles of ethanol fed})} \times 100$$

$$\text{Selectivity}\% = \frac{\text{moles of a certain product}}{\text{moles of total products}} \times 100$$

$$\text{EtOH Conv.}\% = \frac{\text{moles of ethanol converted}}{\text{moles of ethanol fed}} \times 100$$

The thermodynamic analysis in Fig. 1 shows ethanol conversion, yield and selectivity of main products starting from a reactant composition similar to a bio-ethanol stream from biomass fermentation (ethanol-to-water ratio of 1:10). Ethanol conversion is not thermodynamically limited at any temperature. The methanation reaction, which is exothermic, is thermodynamically favored at lower temperatures (below 400 °C). At higher temperatures (above 500 °C) the reverse of this reaction, i.e., steam reforming of methane to CO_2 and H_2 becomes favorable. This would suggest that, if operated in a thermodynamically controlled regime, in order to minimize CH_4 concentration in the product stream, the reaction temperature should be kept as high as possible. However, as shown in Fig. 1, once the temperature is increased above

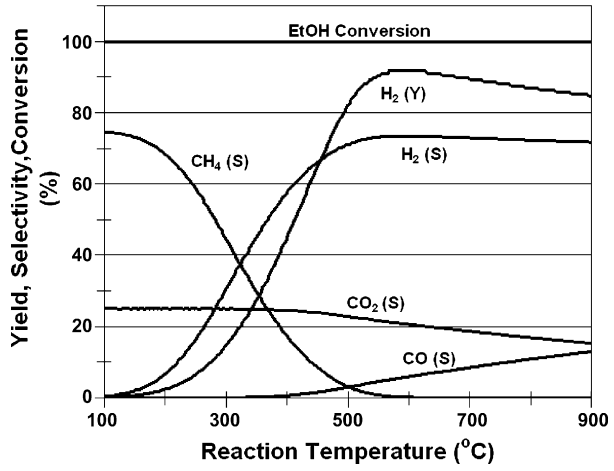

Fig. 1. Product distribution from ethanol steam reforming at thermodynamic equilibrium with EtOH:water = 1:10 (molar), C_{EtOH} = 2.8%, and atmospheric pressure.

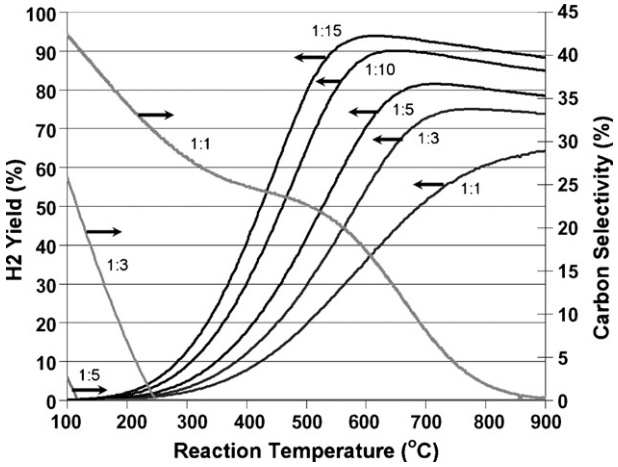

Fig. 2. Effect of EtOH-to-water molar ratio on equilibrium H_2 yield and C selectivity (no dilution).

550 °C, the reverse water-gas shift reaction takes off, i.e., CO formation becomes significant and hydrogen yield decreases. At this ethanol-to-water ratio, there is no solid carbon at the equilibrium state.

Fig. 2 shows the effect of ethanol-to-water molar ratio on H_2 yield. Lower molar ratios of ethanol-to-water can increase the hydrogen yield, since both water-gas shift reaction and CH_4 reforming reactions would shift to the left with increased water concentration. In Fig. 2, solid carbon selectivities for the lowest water concentrations are also included. At high ethanol-to-water ratios, solid carbon deposition becomes thermodynamically favorable, especially at lower temperatures.

The effect of dilution with an inert gas on the equilibrium H_2 yield is shown in Fig. 3. The addition of inert gas increases the equilibrium hydrogen yield at low temperatures and has no effect at high temperatures. At low temperatures, the dominant reaction is the methanation/methane steam reforming. Diluting the system favors the methane steam reforming, and hence we see a difference at low temperatures. At high temperatures, the main reaction is the reverse water-gas shift reaction, which is not affected by dilution, since there is no change in the number of moles with the extent of this reaction. Increased pressure has

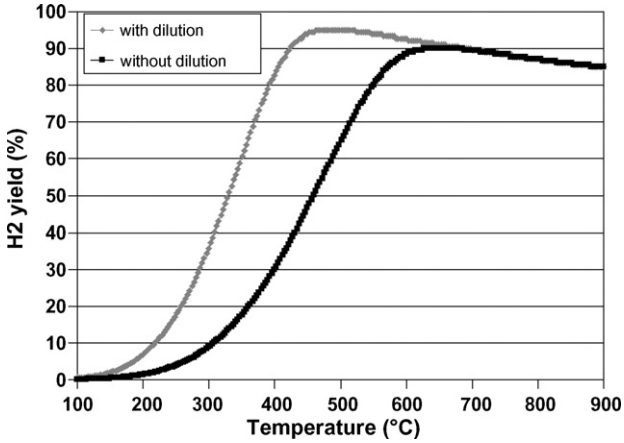

Fig. 3. Effect of dilution on equilibrium hydrogen yield (dilution ratio used: inert:EtOH:H_2O = 25:1:10).

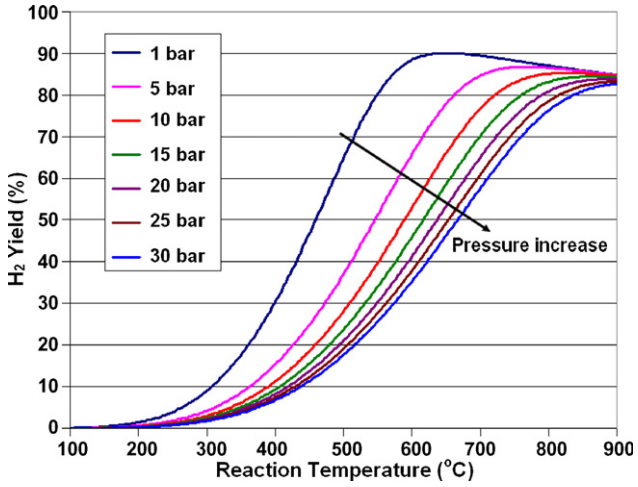

Fig. 4. Effect of pressure on equilibrium hydrogen yield (EtOH:water = 1:10 (molar ratio), no dilution).

a negative influence on hydrogen yield at lower temperatures and no effect at higher temperatures (Fig. 4).

Although it is important to be aware of the thermodynamic limitations, these analyses do not provide any information about the product distribution that would be obtained under kinetically controlled regimes. In this study, care is taken to choose the reaction parameters such that reaction is always controlled by kinetics under thermodynamically favorable conditions.

There have been several studies in the literature on ethanol steam reforming catalysts. Catalysts utilized are mainly Ni, Cu and supported noble metals, like Rh, Pd and Pt [1]. Although supported noble metal catalysts have been shown to have significant activity in 500–600 °C range and high space velocities [2–5], high cost of these metals limits their application. As a less expensive alternative, cobalt-based catalysts have been reported to have superior ethanol steam reforming performance due to their high activity for C–C bond cleavage at temperatures as low as 350–400 °C [6–8]. At these temperatures, researchers have reported good selectivity to CO_2 and H_2 with CH_4 being the only by-product.

An important question in using Co as the active metal is the effect of the support material, which is reported to make a dramatic difference in catalytic performance, including activity, selectivity and stability. Llorca et al. [9] have used *in situ* magnetic characterization of supported cobalt catalysts (1 wt%) to gain insight into active cobalt species for the reaction. A mixture of both metallic and oxidic cobalt species was shown to perform well in the steam reforming reaction. In contrast to this study, recent work by Batista et al. [10] suggested that only Co^0 sites are active for the steam reforming of ethanol. The earlier studies of supported cobalt systems by Haga et al. [11,12] have related catalytic performance to cobalt crystallite size. However, cobalt crystallite size, reducibility and chemical nature, which are important variables during reaction, are directly related to the nature of the support and interactions between cobalt and the support.

Llorca et al. [13] performed studies on MgO, Al_2O_3, SiO_2, TiO_2, V_2O_5, ZnO, La_2O_3, CeO_2, and Sm_2O_3. Although cobalt catalysts supported on these oxides showed comparable activity, the product distribution was significantly different. While conventionally a metal oxide support is used in conjunction with Ni or Co to increase the surface area of the exposed metal, the support almost always plays a role in intermediate steps in ethanol reforming reactions [8,11,14]. The support can often act as a site for reactant adsorption. Some sites on the support can induce side reactions in steam reforming. For instance, acid sites on alumina are known to be active for ethanol dehydration to ethylene, a common by-product in ethanol steam reforming [15].

Another important aspect of these catalyst/support systems is the effect the support has on the reducibility and ultimate dispersion of the active metal and the resulting influence on activity. In many supported cobalt systems, especially those at higher cobalt loadings, all of the cobalt cannot be reduced to the metallic state at reasonable temperatures. Jacobs et al. [16] have studied supported cobalt on Al_2O_3, TiO_2, SiO_2, and ZrO_2-modified SiO_2 for optimization in the Fischer–Tropsch reaction. Significant support interactions were observed in the order $Al_2O_3 > TiO_2 > SiO_2$. The cobalt species strongly interacting with the support required harsher reduction conditions. Promotion with small amounts of Ru and Pt metals was able to aid in the reduction of Co species that were strongly interacting with the support. Another factor investigated by researchers is the type of precursor and support materials. Kraum and Baerns [17] found that, depending on the precursor material, the interactions between precursors and supports during catalyst preparation and treatment differed, which resulted in differences in cobalt dispersion. Such parameters are taken advantage of in the work of Iglesia et al. [18] who have used novel molten nitrate impregnation to achieve as high as 50% cobalt weight loadings.

Ho and Su [19] studied silica-supported cobalt system by using different solvents to dissolve the Co precursor. Compared with aqueous solution, ethanol impregnation onto the support yields smaller uniformly distributed Co particles on the surface and less metal sintering happens at high temperature. Kaddouri and Mazzocchia [20] investigated Co/SiO_2 and Co/Al_2O_3 for bio-ethanol reforming. They examined both impregation and sol–gel preparation methods and studied metal and support interactions as well as selectivity and product distributions in two systems. Vargas et al. [21] examined Ce–Zr–Co fluorite-type as a catalyst for ethanol steam reforming. They found that after *in situ* controlled partial reduction of the catalysts at 440 °C, part of the Co was reduced into nano-particles of Co^0, which were active and selective for reactions under 440 °C while with further increase in reaction temperature (540 °C), catalysts underwent a deeper reduction, leading to deactivation.

In this study, we examined Co catalysts on different supports including alumina, titania and zirconia. Our research is focused on interactions between metal and supports, nature of active sites, and surface intermediates during reaction. An incipient wetness impregnation method was used for catalyst preparation. Catalysts were tested for their activity in ethanol steam

reforming using an in-house-built reactor system. Characterization was performed using TGA, H_2 chemisorption, temperature-programmed reaction (TPRxn), laser Raman spectroscopy, and DRIFTS. It was found that zirconia-supported cobalt catalysts gave the best cobalt dispersion. Zirconia was chosen as the support for further studies. DRIFTS was used to investigate surface interactions with reactant molecules during reaction.

2. Experimental

2.1. Catalysts preparation

Supported cobalt catalysts with different weight loadings were prepared in the air by incipient wetness impregnation from cobalt (II) nitrate hexahydrate (Aldrich 99.999%) aqueous solutions. The supports used and their corresponding surface areas and pore volumes were γ–Al_2O_3 (199 m^2/g, 0.44 cm^3/g), TiO_2 (59 m^2/g, 0.11 cm^3/g), ZrO_2 (31 m^2/g, 0.21 cm^3/g), all of which were purchased from Saint Gobain. The support pellets were ground and then sifted through a 100–150 mesh. The sifted supports were then calcined for 3 h under air at 500 °C prior to impregnation. After repeating impregnation and drying in an oven overnight at approximately 95 °C as many times as determined by the pore volume of each support, some of the resulting samples were calcined at 400 °C for 3 h under air and stored for use, the rest were kept uncalcined for thermogravimetric analysis.

2.2. Catalysts characterization

2.2.1. TGA

The TGA experiments were performed on a Perkin-Elmer TGA7 instrument. The system is capable of quantitatively measuring the change in mass of a sample as a function of temperature up to 1000 °C. The change in mass is then related to the changes taking place in the catalyst during calcination. For each sample prepared, air was flown through the TGA at 25 mL/min as the temperature was ramped at 10 °C/min.

2.2.2. H_2 Chemisorption

The volumetric measurement of H_2 chemisorption was conducted using a Micromeritics ASAP 2010 Chemisorption system. Prior to adsorption measurements, calcined samples were reduced *in situ* under 5% H_2/He at the desired reduction temperature (in this case 400 °C) for 3 h followed by evacuation to 10–5 mmHg and cooling down to 35 °C. The adsorption isotherms were measured at equilibrium pressures between 50 and 500 mmHg. The first adsorption isotherm was established by measuring the amount of H_2 adsorbed as a function of pressure. After completing the first adsorption isotherm, the system was evacuated for 1 h at 10–5 mm Hg. Then a second adsorption isotherm was obtained. The amount of probe molecule chemisorbed was calculated by taking the difference between the two isothermal adsorption amounts.

2.2.3. Temperature-programmed reaction

TPRxn experiments were performed using the Cirrus MS (MKS Instruments, 1–300 amu) to monitor reactor outlet composition. The samples were pre-reduced (5% H_2/He, 30 mL/min) at 350 °C and cooled to room temperature under helium. The feed for the TPRxn experiments was provided by saturating helium steams with water and ethanol in a double-bubbler arrangement to provide an ethanol:water molar ratio of 1:10. After stabilization of water and ethanol signals, the temperature was ramped at 10 °C/min.

2.2.4. Raman spectroscopy

The Raman spectroscopy was performed using a 514.5 nm argon ion laser on a Laser Raman spectrometer (Kaiser) with a 1000× microprobe. The three catalysts tested were zirconia-supported Co catalysts with different Co loadings: 5, 10 and 15 wt%. The spectra of ZrO_2 and Co_3O_4 were also taken as the standards for crystal phase identification.

2.2.5. DRIFTS

The DRIFTS experiments were performed on a Bruker IFS66 DRIFT spectrometer equipped with a MCT detector. The catalyst used for the DRIFTS experiment was the 10% Co/ZrO_2 calcined at 400 °C for 3 h. The catalyst was pre-reduced *in situ* at 350 °C while flowing 5% H_2/He for 2 h. An ethanol and water mixture (1:10 ratio) was then allowed to adsorb onto the catalyst surface for one hour. The system was then flushed with helium. The spectra were taken after stabilization at each temperature.

2.3. Catalytic tests

A reactor system (shown in Fig. 5) has been designed and constructed for BESR and oxidative ethanol steam reforming (OESR), for catalytic performance evaluation and kinetic studies. The synthesized feed with designated molar ratio of water to ethanol or the crude ethanol solution obtained from the fermentation of biomass can be sent into the system either through bubblers or through the combination of a HPLC pump and an evaporator. The sample pretreatment, reaction, and regeneration steps have been integrated into one system. The reactant and product streams can be analyzed online by either being directly injected into a GC or first passing through a condenser and then being sent into the GC separately. Analysis methods have been developed to identify and quantify the reaction products. An on-line Cirrus mass spectrometer (MKS Instruments, 1–300 amu) has also been installed for additional product analysis or for isotopic labeling studies.

The catalytic studies of the BESR were performed in a tubular reactor (4 mm internal diameter). The catalyst (250 mg) was added for each run. The feed stream comprised of a gaseous mixture of nitrogen used as internal standard, helium used as carrier gas, water, and ethanol vapors generated from bubblers heated to their respective designated temperatures, calculated by Antoine equation. The molar ratio of ethanol to water can be adjusted by controlling the bubbler temperatures and the carrier gas flow rates.

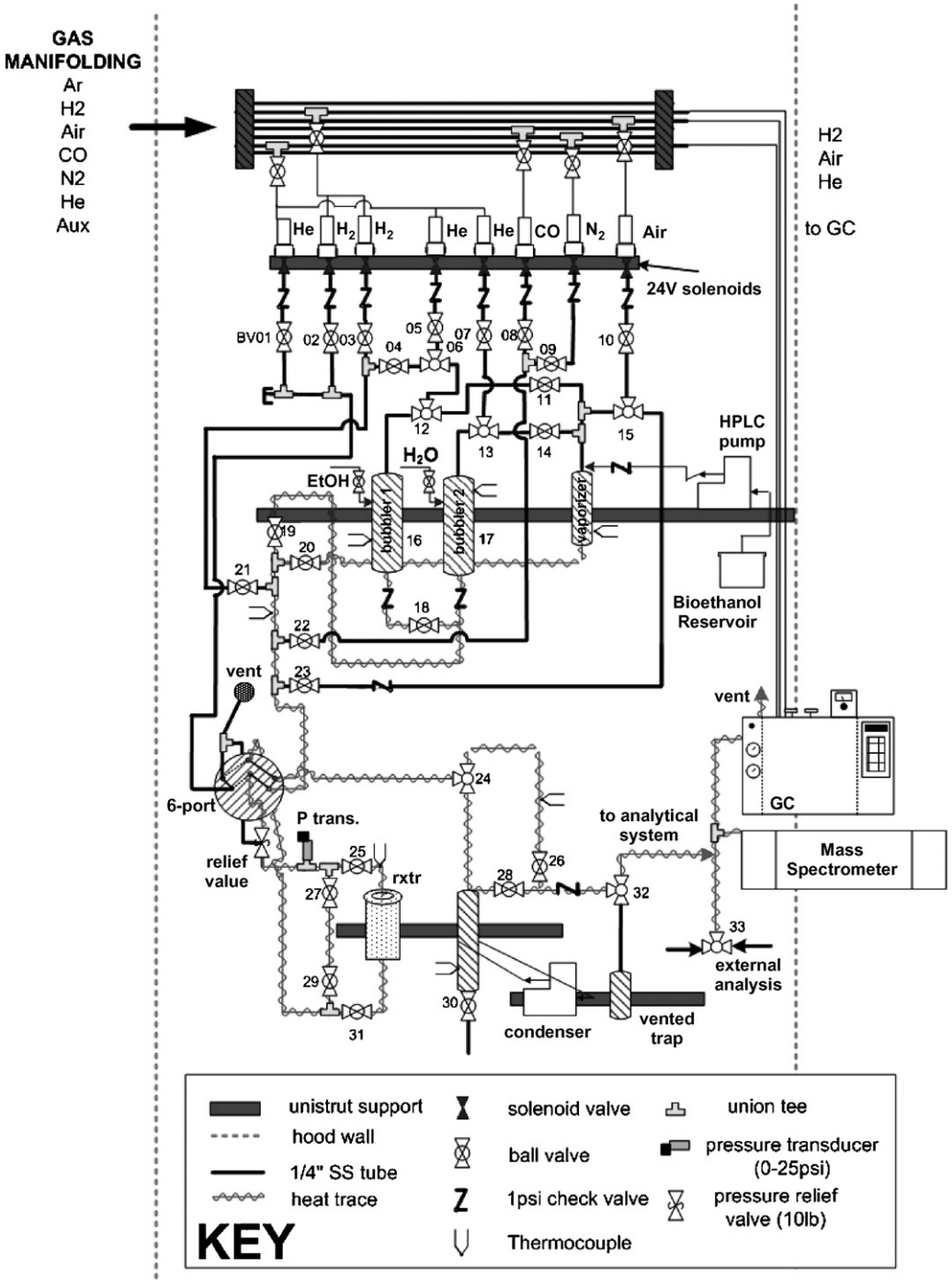

Fig. 5. Schematic diagram of the reactor system for the bio-ethanol steam reforming.

All catalysts were first pretreated at 300 °C for 30 min under He and then reduced *in situ* at 400 °C for 2 h under 5% H_2/He. Subsequently the catalytic performances were tested in the temperature range of 300–550 °C, in 50 °C increments. The catalyst was held at each temperature for at least 2 h. At the end of the catalytic test, the flow of EtOH + H_2O was stopped and the catalyst was cooled under He stream.

The analysis of the reactants and all the reaction products was carried out online by gas chromatography (Shimadzu Scientific 2010). Analysis was done using two different detectors and the separation was achieved using two different sample injection loops/valves and two analysis lines: The first line consisted of a Carboxen column and a 5 Å molecular sieve column connected in series in a column isolation scheme. This combined column arrangement was used in conjunction with a pulse discharge helium ionization detector (PDHID). The second line was a separate 30 m-long Q-Plot column used with a methanizer and a flame ionization detector (FID) to allow detection of CO down to 10 ppm. Helium was used as the carrier gas for both of the analysis lines. All the carbon containing products can be separated by the Q-Plot column and detected by FID. PDHID can detect all the products in the

stream, including CO, CO_2, and H_2. Response factors for all products were obtained and the system was calibrated with appropriate standards before each catalytic test.

The H_2 yield and ethanol conversion were defined the same as those used for thermodynamic analysis given in the Introduction section.

3. Results and discussion

3.1. TGA

The changes occurring during the calcination of catalysts were studied through TGA. Fig. 6 shows the derivative of the mass (DTG) profile obtained during calcinations. The TGA profiles for the cobalt catalysts supported on titania and alumina are very similar. They each have only one sharp peak corresponding to the weight loss associated with decomposition/oxidation of nitrates and precursor materials from the catalyst. However, TGA results over the zirconia-supported sample show that there is greater interaction between the support and the metal as seen through additional mass change features at higher temperatures.

3.2. Raman

Fig. 7 shows the Raman spectra of Co/ZrO_2 with different Co loadings after calcination. Compared with ZrO_2 (monoclinic) spectra, it is evident that the surface of ZrO_2 in all the samples has been covered by cobalt particles even if the cobalt loading is as low as 5 wt%, resulting in the absence of ZrO_2 characteristic peaks in the sample spectra. The only Raman features visible are those of CO_3O_4 as identified by the Co_3O_4 standard spectrum.

3.3. H_2 Chemisorption

As suggested by the TGA results, interactions between the cobalt metal and the support varied significantly, depending on the support material. The support effects are likely to result in differences in cobalt crystal size and dispersion on the surface after reduction. H_2 chemisorption was used to determine the ratio of exposed metal atoms to total metal atoms (dispersion (%)). The dispersion calculation is based on a stoichiometry of 1 H atom per metal atom. As shown in Fig. 8, ZrO_2 supported catalysts gave the highest metal dispersion compared with the alumina and titania supports. The lowest cobalt dispersion was observed for the titania-supported catalyst.

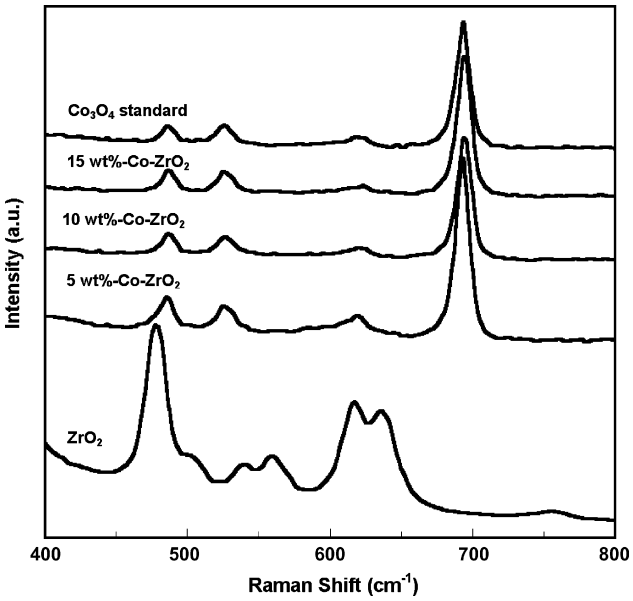

Fig. 7. Raman spectra of ZrO_2 support, C_3O_4 and Co/ZrO_2 with different Co loading levels.

3.4. DRIFTS

The reaction intermediates on the surface of 10% Co/ZrO_2 were investigated through DRIFTS. The evolution of surface species along with the increase of reaction temperature is shown by DRIFT spectra shown in Fig. 9. At room temperature, the band located at 1653 cm^{-1} [22] is due to the O–H scissoring coming from adsorbed water. The monodentate and bidentate ethoxide (drawn on the top left in Fig. 9) is formed on the sample surface, as identified by the CH_3 bending (1458, 1385 cm^{-1}) and CCO stretching (1169, 1105, 1063) vibrations due to ethanol adsorption [23,24]. Initial temperature increase

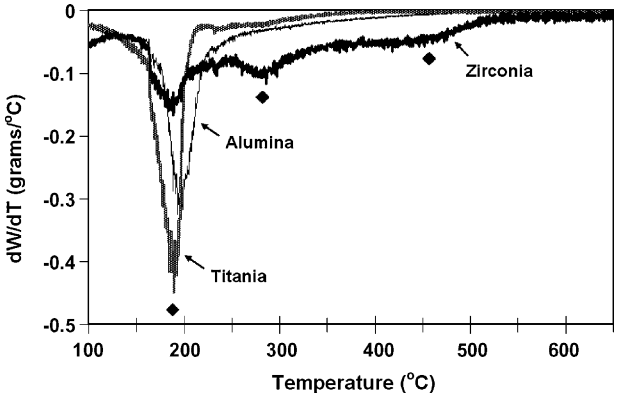

Fig. 6. DTG profiles of 10% Co supported on ZrO_2, γ-Al_2O_3, TiO_2 during calcination under air.

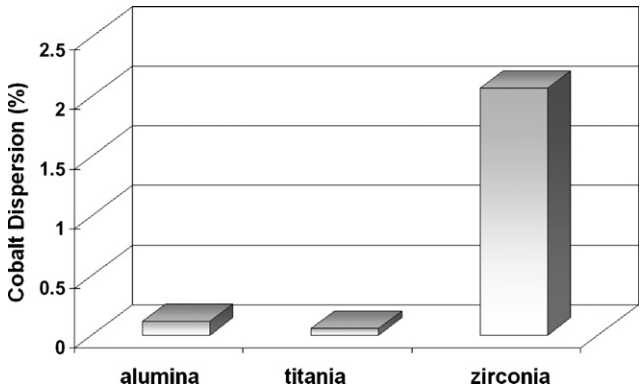

Fig. 8. Cobalt dispersion measured through H_2 chemisorption over different supports.

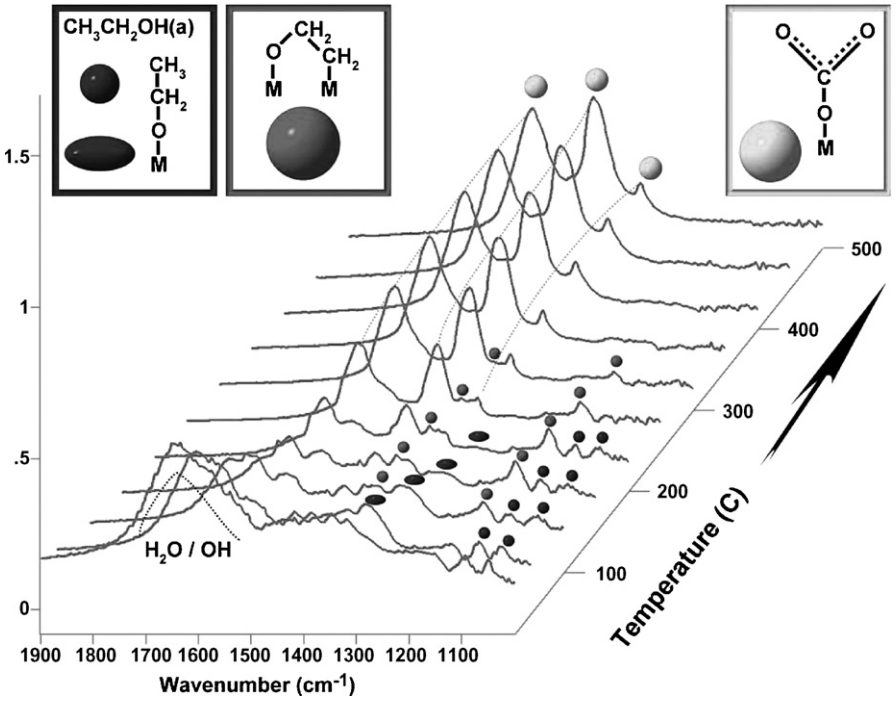

Fig. 9. *In situ* DRIFT spectra of 10% Co/ZrO_2 after adsorbing ethanol and water vapor (1:10, molar ratio) at room temperature.

favors the ethoxide adsorbed in bidentate form. The bands characteristic of ethoxy species subsequently disappeared with the further increase in temperature due to the BESR reaction happening. The presence of surface acetate species has been identified at 1569 cm^{-1} (ν_{assym}(COO)), 1429 cm^{-1}(ν_{sym}(-$_{sym}$(COO)), and 1380 cm^{-1} ($\delta(CH_3)$) [25]. As seen in Fig. 9, these species could first evolve to monodentate carbonate [26,27] as an intermediate, then dissociate into gas molecules, such as CO, CO_2 and CH_4.

3.5. Activity tests

Fig. 10 shows some of the preliminary results presented in terms of ethanol conversion rates per catalyst surface area. The H_2O:EtOH:inert ratio is 3:1:6 and the GHSV is 150,000 h^{-1}. The results are interesting in showing the importance of the support on the performance of the catalyst. As shown, zirconia-supported catalyst has the highest activity based on equal surface area while alumina- and titania-supported cobalt catalysts show much lower activities (Fig. 10a). When hydrogen yields are compared (Fig. 10b), it is seen that only the zirconia-supported catalyst shows appreciable yields of hydrogen (at 450 and 500 °C) while the yields over the other two catalysts are much lower.

Although data not shown here, the alumina-supported catalyst showed selectivity mainly to ethylene, which is not surprising considering the many reports that show the acidity of alumina contributing to the formation of ethylene and coke. The titania and alumina-supported catalysts also showed selectivity to acetaldehyde while the zirconia-supported catalysts exhibited very low acetaldehyde formation. The cobalt–zirconia system presents itself as promising for hydrogen production

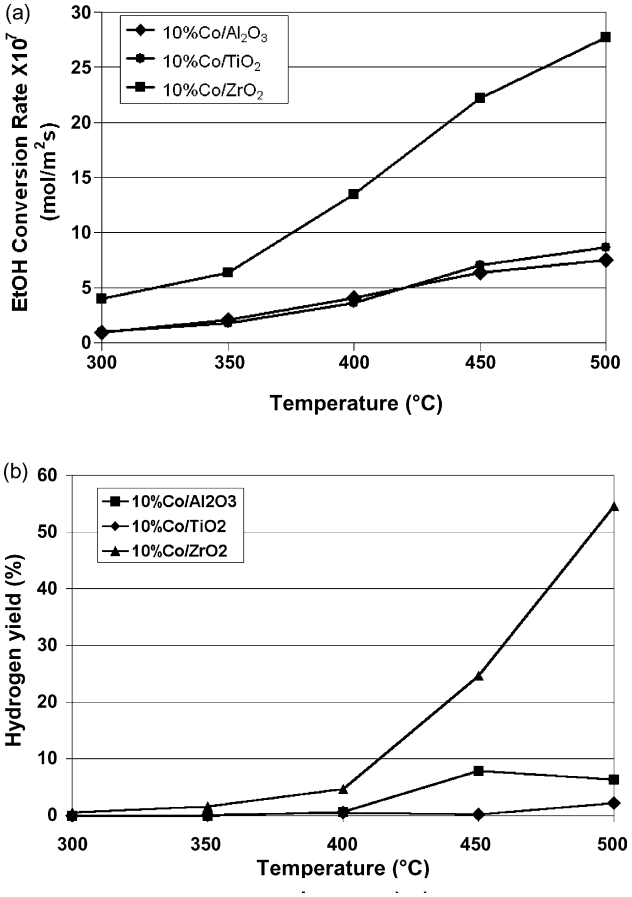

Fig. 10. Steady state reaction results for 10% Co catalysts on different supports. Reaction conditions: H_2O:EtOH:inert = 3:1:6 (molar ratio), GHSV = 150,000 h^{-1} (a) ethanol conversion rates (b) H_2 yields.

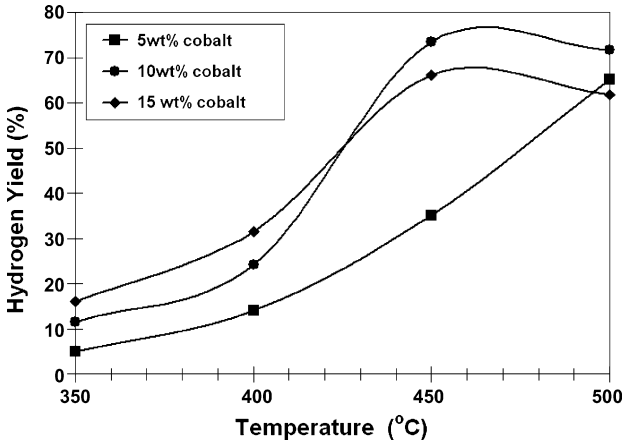

Fig. 11. Effect of catalyst loading on H_2 yield over Co/ZrO_2 catalysts.

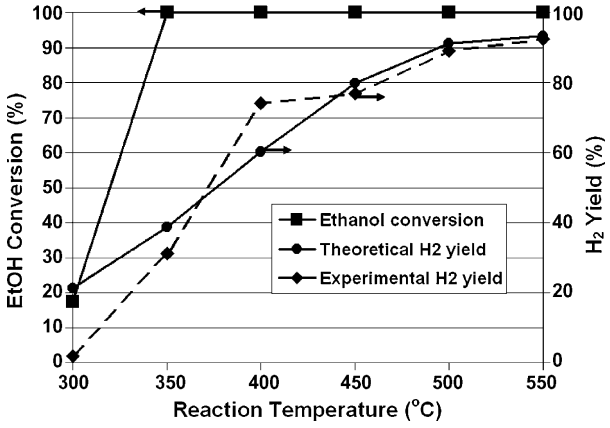

Fig. 13. Steady state reaction data for 10% Co/ZrO_2. Reaction conditions: H_2O:EtOH:inert = 10:1:75 (molar ratio), GHSV = 5000 h^{-1}.

from bio-ethanol steam reforming. Later in our work, zirconia-supported cobalt catalysts were chosen as the focus of study.

The effect of Co loading on ZrO_2 support was also examined. The experimental parameters used for these reactions were 4% EtOH, EtOH/H_2O ratio = 1:10, and GHSV = 250,000 h^{-1}. A comparison of the H_2 yields is presented in Fig. 11. A loading of 10% is found to give the highest H_2 yield at temperatures above 400 °C. The highest yield obtained over this catalyst is 75% at 450 °C.

The TPRxn experiments for the 10% Co/ZrO_2 catalyst calcined at 400 °C and reduced at 350 °C for 2 h have been performed to explore the product distribution under unsteady state. The reaction mixture consisted of 3% EtOH and a EtOH:H_2O ratio of 1:10. The GHSV was 15000 h^{-1}. The results are shown in Fig. 12. The light-off temperature for ethanol conversion is below 300 °C and by 430 °C, 100% ethanol conversion is achieved. The H_2 signal rises sharply up to 430 °C and shows a slower increase up to 600 °C. There is a decrease in H_2 signal at higher temperatures. Methane formation is limited to a temperature window between 300 and 430 °C. The CH_3COCH_3 formation is seen between 350 and 400 °C. The CO signal shows multiple maxima, possibly due to different reactions involved in its formation, including ethanol decomposition, CH_4 reforming and reverse water-gas shift reaction. The decrease seen in the CO_2 signal at temperatures above 450 °C is also likely to be due to reverse shift reaction. Other species observed include C_2H_6 or C_2H_4 (C_2) and diethyl ether, both of which are in very small quantities. TPRxn experiments are informative in demonstrating the complex reaction network involved in the ethanol steam reforming and how the product distribution is determined by the many competing reactions that become important at different temperatures.

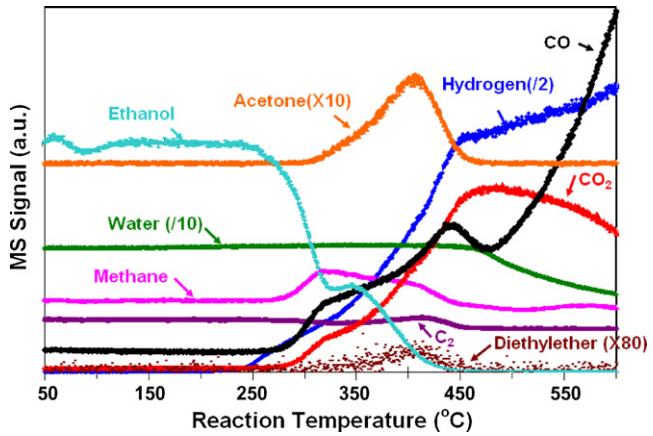

Fig. 12. Concentration profiles of different products during TPRxn over 10% Co/ZrO_2.

Fig. 13 shows the steady state reaction results obtained over the 10% Co/ZrO_2 catalyst at a lower GHSV. The most striking result is the high H_2 yields that reach 75% at temperatures as low as 400 °C. At 550 °C, a H_2 yield of 92% is achieved, which is equivalent to 5.5 mol of H_2 produced per mol of ethanol fed. Compared with the equilibrium value obtained from thermodynamic calculation, 400 °C gives much higher experimental hydrogen yield, confirming that the reaction is kinetically controlled at lower temperatures. However, above 450 °C, the H_2 yield is very close to the equilibrium yield, indicating that thermodynamic limitation begins taking control at higher temperatures. In addition, ethanol can be fully converted at temperatures as low as 350 °C. What is also worth noting is that at temperatures above 475 °C, the only other product besides hydrogen and CO_2 is CO, making H_2 the only H-containing product.

4. Conclusions

Initial studies on cobalt-based catalysts supported γ-Al_2O_3, TiO_2, ZrO_2 supports have shown promising results for BESR reaction. As determined by the H_2 chemisorption studies, ethanol conversion is found to correlate closely with metal dispersion and hence, the metallic Co sites. The product distribution, on the other hand, is determined by a complex network of competing reactions, including BESR, methanation, WGS, dehydration, and dehydrogenation. Among the supports studied, zirconia is shown to provide the highest metal dispersion and the highest H_2 yield. H_2 yields as high as 92% (5.5 mol of H_2 per mole of ethanol fed) are achieved over a 10% Co/ZrO_2 catalyst at 550 °C.

Acknowledgement

We gratefully acknowledge the funding from the U.S. Department of Energy through the grant DE-FG36-05GO15033.

References

[1] A. Haryanto, S. Fernando, N. Murali, S. Adhikari, Energy Fuels 19 (2005) 2098–2106.
[2] S. Cavallaro, V. Chiodo, S. Freni, N. Mondello, F. Frusteri, Appl. Catal. A: Gen. 249 (2003) 119–128.
[3] D. Liguras, D. Kondarides, X. Verykios, Appl. Catal. B: Environ. 43 (2003) 345–354.
[4] C. Diagne, H. Idriss, A. Kiennemann, Catal. Commun. 3 (2002) 565–571.
[5] S. Cavallaro, Energy Fuels 14 (2000) 1195–1199.
[6] J.R. Mielenz, Curr. Opin. Microbiol. 4 (2001) 324–329.
[7] J. Llorca, P.R. de la Piscina, J.-A. Dalmon, J. Sales, N. Homs, Appl. Catal. B: Environ. 43 (2003) 355–369.
[8] J. Llorca, N. Homs, J. Sales, P.R. de la Piscina, J. Catal. 209 (2002) 306–317.
[9] J. Llorca, J.A. Dalmon, P.R. de la Piscina, N. Homs, Appl. Catal. 243 (2003) 261–269.
[10] M.S. Batista, K.S. Santos, E.M. Assaf, J.M. Assaf, Ticianelli, J. Power Sources 124 (2003) 99–103.
[11] F. Haga, T. Nakajima, H. Miya, S. Mishima, Catal. Lett. 48 (1) (1997) 223–227.
[12] F. Haga, T. Nakajima, S. Yamashita, S. Mishima, Kinet. Catal. Lett. 63 (1998) 253–259.
[13] J. Llorca, P.R. de la Piscins, J. Sales, N. Homs, Chem. Commun. (2001) 641–642.
[14] F. Auprete, C. Descorme, D. Duprez, Catal. Commun. 3 (2002) 263–267.
[15] F. Marino, M. Boveri, G. Baronetti, M. Laborde, Int. J. Hydrogen Energy 26 (2001) 665–668.
[16] G. Jacobs, T.K. Das, Y. Zhang, J. Li, G. Racoillet, B.H. Davis, Appl. Catal. A: Gen. 233 (2002) 263–281.
[17] M. Kraum, M. Baerns, Appl. Catal. A: Gen. 186 (1999) 189–200.
[18] E. Iglesia, S.L. Soled, J.E. Baumgartner, S.C. Reyes, J. Catal. 153 (1995) 108–122.
[19] S.W. Ho, Y.S. Su, J. Catal. 168 (1997) 51–59.
[20] A. Kaddouri, C. Mazzocchia, Catal. Commun. 5 (2004) 339–345.
[21] J.C. Vargas, S. Libs, A.C. Roger, A. Kiennemann, Catal. Today 107–108 (2005) 417–425.
[22] S.Yu. Venyaminov, F.G. Prendergast, Anal. Biochem. 248 (1997) 234–245.
[23] A. Erdöhelyi, J. Raskó, T. Kecskés, M. Tóth, M. Dömök, K. Baán, Catal. Today 116 (2006) 367–376.
[24] J.M. Guil, N. Homs, J. Llorca, P.R. Piscina, J. Phys. Chem. B 109 (2005) 10813–10819.
[25] J. Raskó, M. Dömök, K. Baán, A. Erdöhelyi, Appl. Catal. A: Gen. 299 (2006) 202–211.
[26] L.V. Mattos, F.B. Noronha, J. Power Sources 152 (2005) 50–59.
[27] L.V. Mattos, F.B. Noronha, J. Catal. 233 (2005) 453–463.